Materials Physics and Mechanics 35 (2018) 155-166 Received: December 7, 2017

MULTILAYERED SCROLLS OF CARBON NANORIBBONS

A.V. Savin[1], S.V. Dmitriev[2,3], E.A. Korznikova[2*], A.A. Kistanov[4]

[1] Institute of Physical Chemistry, RAS, Kosygin St. 4, 119991 Moscow, Russia

[2] Institute for Metals Superplasticity Problems, RAS, Khalturin St. 39, 450001 Ufa, Russia

[3] National Research Tomsk State University, Lenin Ave. 36, 634050 Tomsk, Russia

[4] Nanyang Technological University, Nanyang Ave. 50, 639798, Singapore

[*]e-mail: elena.a.korznikova@gmail.com

Abstract. Possible equilibrium states of multilayered carbon nanoribbons are found using the chain model moving on a plane previously proposed by the authors. For very short nanoribbons only flat multilayered structures are possible, while for sufficiently long nanoribbons the lowes energy have nanoscrolls with folded structures having intermediate value of energy. Dependencies of the internal and external radii of the scrolls, as well as the number of coils on the nanoribbon length are calculated. It is found that the radial thermal espansion coefficient of nanoscrolls is two or even three orders of magnitude larger than the linear thermal expansion coefficient of diamond. Thus, carbon nanoscrolls can be used to make very sensitive temperature sensors.

Keywords: graphene; chain model; scrolls; thermal expansion.

1. Introduction

Intensive studies on mechanical, physical and nonlinear properties of graphene sheets and nanoribbons motivated by their outstanding combination of properties and application perspectives are being conducted recently [1-7]. Of particular interest are also their secondary structures (e.g. scrolls and folds), stability of which is provided by the presence of weak non valence van der Waals interactions, because they can have functional properties different from flat conformations [8]. Scrolling or folding of graphene sheets or nanoribbons can result in improving some of their functional properties and enable novel applications. For instance, graphene nanoscrolls exhibit tunable transport [9] supercapacitance, and enhanced hydrogen storage [8]. The possibility of the formation of graphene scrolls during the abrasion of the graphite lubricant was reported as early as in [10,11]. Recently a number of experimental methods of obtaining scroll structures from flat graphite and graphene have been developed. Among these methods one can mention wet chemistry technique [12], fabrication of carbon nanoscrolls in isopropyl alcohol solution from graphene positioned on SiO_2/Si substrates [13] and ultrasonic treatment of intercalated graphite [14]. Although assembly of nanoribbons into secondary structures since recently is possible, current methods suffer from limited control of their atomic structure [15]. Application of molecular dynamics and ab-initio simulation methods to scrolled graphene revealed that they can be used as electroactuators [16] or gigahertz breathing oscillators [14] and some other electronic devices [9,17]. The large number of interacting atoms in such structures imposes significant restrictions on the modeling of their dynamics. A well known mechanical approach to simplify the problem is constructing of effective models with reduced number of degrees of freedom. In many cases this is not a simple task and pecularities of microstructure should be carefully taken into account. In the classical

http://dx.doi.org/10.18720/MPM.3512018_18

works by Maugin and Aero generalized continuum models with microscopic degrees of freedom have been developped [18-20]. In should be noted that conduction of long-term simulations of large scale secondary graphene structures using full atomic models can be realized only for relatively short nanoribbons. In order to solve this problem in [21-25] a simple model of molecular chain moving in the plane, that takes into account the longitudinal and flexural rigidity of carbon nanoribbon, has been proposed. The model provides a possibility to investigate dynamics of extended nanoribbons and their secondary structures (multi-folds, scrolls, etc.). Stable static configurations of secondary structures and their dynamics have been studied in frame of this model [21-25]. Present paper deals with possible configurations of multilayer carbon nanoribbons investigated by means of our model.

2. Chain model of single layered carbon nanoribbon

Single layered graphene nanoribbon is a constant width ribbon cut from a flat sheet of graphene. Graphene is an elastically isotropic material and due to this fact the longitudinal and flexural rigidity of the nanoribbon shows a weak dependence on its chirality. For definiteness we consider the structure of zigzag nanoribbon shown in Fig. 1 (a). In the ground state the flat nanoribbon lies in the *xz* plane with zigzag direction oriented along *x* axis. This nanoribbon is a periodic structure with lattice distance $a = r_0 \cos(\pi/6)$, where $r_0 = 0.1418$ nm is the equilibrium length of the C-C valence bond. Translational cell of the structure is formed by atomic rows parallel to the *z* axis. Consider the movements of the nanoribbon in which the atoms of each translational cell move as a rigid body in the *xy* plane, but not in *z* direction. Then the atoms of each cell can be represented by one efficient particle able to move in the *xy* plane. In this case, the movement of the nanoribbon can be presented as the movement of the chain of effective particles, see. Fig. 1 (b). Thus, stretching and bending movement of the nanoribbon can be described as the motion of chain of particles in the *xy* plane. The chain model is shown schematically in Fig. 1 (c).

The chain Hamiltonian can be presented as:

$$H = \frac{1}{2}\sum_{n=1}^{N} M\left(\dot{x}_n^2 + \dot{y}_n^2\right) + \sum_{n=1}^{N-1} V(r_n) + \sum_{n=2}^{N-1} U(\theta_n) + \sum_{n=1}^{N-4}\sum_{k=n+4}^{N} W_i(r_{nk}), \quad (1)$$

where (x_n, y_n) are the coordinates of *n*-th particle, $M = 12m_p$ is carbon atom mass ($m_p = 1.6603\times10^{-27}$ kg is mass of the proton). The potential

$$V(r) = \frac{K}{2}(r-a)^2, \quad (2)$$

describes the longitudinal rigidity of the chain. The distance between adjacent particles is $r_n = |v_n|$, where the vector $v_n = (x_{n+1} - x_n, y_{n+1} - y_n)$ connects *n*-th and (n+1)-th particles. The angular potential

$$U(\theta) = \varepsilon[\cos(\theta) + 1] \quad (3)$$

describes the bending stiffness of the chain, where cosine of *n*-th "valence" angle is $\cos(\theta_n) = -(v_{n-1}, v_n)/r_{n-1}r_n$. The potential $W_i(r_{nk})$, (*i*=1,2) describes weak van der Waals interactions between *n*-th and *k*-th particles positioned at the distance $r_{nk} = \sqrt{(x_k - x_n)^2 + (y_k - y_n)^2}$ (*i*=1 for odd difference *k*-*n* and *i*=2 in the cases of even difference). The potential W_i is vitally important for modelling of nanoribbon secondary structures. Interaction potential parameters (2), (3) have been defined previously in [18] by means of analysis of carbon nanoribbon dispersion curves. The fitted rigidity is *K*=405 N/m and the energy is ε=3.50 eV. With this values longitudinal and bending rigidity of the chain coincides with the carbon nanoribbon rigidity. Note that the standard set of interatomic potentials developed in [26] was used in the full-atomic calculations.

This potential has been succesfully used in simulations of nonlinear lattice dynamics of graphene and other sp^2 structures [27-29].

The interaction potential of remote particles $W_i(r)$ can be defined as the sum of Lennard-Jones interaction potentials of carbon atoms belonging to appropriate elementary cells of the nanoribbon. It was shown previously in [21] that non-valence interactions of chain particles can be effectively described by means of modified Lennard-Jones potential:

$$W_i(r) = 4\varepsilon_i\left[\left(\sigma_i / f(r)\right)^{12} - \left(\sigma_i / f(r)\right)^{6}\right],$$
$$f(r) = r_i (r / r_i)^{\alpha_i}, \quad r_i = 2^{1/6}\sigma_i, \quad i = 1,2, \tag{4}$$

with parameters ε_1=0.008652 eV, σ_1=0.31636 nm, α_1=0.86 for index i=1 and ε_2=0.008029 eV, σ_2=0.32607 nm, α_2=0.90 for index i=2.

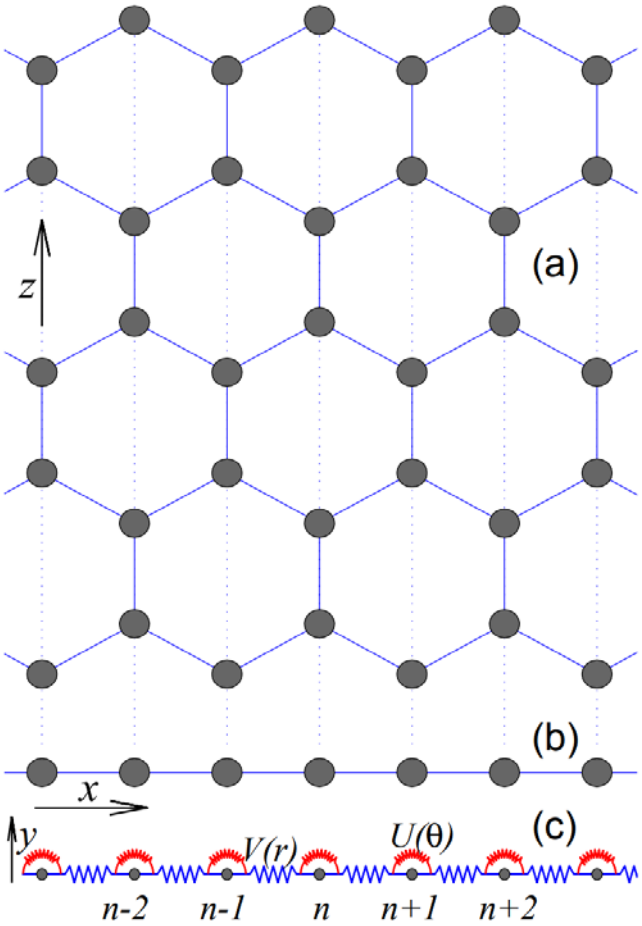

Fig. 1. (*a*) Nanoribbon with zigzag orientation along *x* axis and (*b*) its chain model. Particles of the chain are numbered by index *n*. (*c*) Chain of particles on the *xy* plane describing the longitudinal and bending rigidity of carbon nanoribbon. The potential $V(r)$ describes the longitudinal rigidity and the angular potential $U(\theta)$ defines the nanoribbon bending rigidity.

3. Multilayered nanoribbon model

In case of *k* layers of graphene nanoribbons, a system of *k* parallel chains is considered. The Hamiltonian of *k*-layered nanoribbon can be presented as:

$$H = \sum_{j=1}^{k}\left[\frac{1}{2}\sum_{n=1}^{N-1} M(\dot{x}_{n,j}^2 + \dot{y}_{n,j}^2) + \sum_{n=1}^{N-1} V(r_{n,j}) + \sum_{n=2}^{N-1} U(\theta_{n,j}) + \sum_{n=1}^{N-4}\sum_{k=n+4}^{N} W(r_{n,j;k,j})\right]$$
$$+ \sum_{j=1}^{k-1}\sum_{l=j+1}^{k}\sum_{n=1}^{N}\sum_{m=1}^{N} W_i(r_{n,j;m,l}), \tag{5}$$

where the vector $u_{n,j}=(x_{n,j},y_{n,j})$ sets the coordinates of n-th particle of j-th chain. The first term of the sum (5) sets the energy of separated k chains consisting of N elements each, and the second one defines the energy of interaction between chains. The distance $r_{n,j}=\left|v_{n,j}\right|$, where the vector $v_{n,j}=u_{n+1,j}-u_{n,j}$. The valent angle cosine is $\cos(\theta_{n,j})=-(v_{n-1,j},v_{n,j})/r_{n-1,j}r_{n,j}$, where the distance $r_{n,j;m,l}=\left|u_{n,j}-u_{m,l}\right|$.

In order to find the stationary state of multilayered nanoribbon the following minimum value problem should be solved:

$$E=\sum_{j=1}^{k}\left[\sum_{n=1}^{N-1}V(r_{n,j})+\sum_{n=2}^{N-1}U(\theta_{n,j})+\sum_{n=1}^{N-4}\sum_{k=n+4}^{N}W(r_{n,j;k,l})\right]$$
$$+\sum_{j=1}^{k-1}\sum_{l=n\backslash j+1}^{k}\sum_{n=1}^{N}\sum_{m=1}^{N}W_i(r_{n,j;m,l})\rightarrow\min:\left\{u_{n,j}\right\}_{n=1,j=1}^{N,k}, \quad (6)$$

i. e. one should perform the minimisation of the potential energy of k chain system with respect to coordinates of the particles, $\left\{u_{n,j}\right\}_{n=1,j=1}^{N,k}$. Let us consider $\left\{u_{n,j}^{0}\right\}_{n=1,j=1}^{N,k}$ as the solution to the minimum value problem (6). In this case, the normalised energy (energy per one particle) of corresponding stationary structure can be defined as $E_0=E(u_{n,j}^{0})/Nk$. The solution of the minimum problem (6) has been performed by means of adjacent gradient method.

Performing energy minimization of different initial chain configurations one can obtain the whole variety of possible stationary states of the system consisting of k chains. Namely this can be a flat multilayered structure (see Fig. 2, c and f), different fold types (see Fig. 2, b and e) and different types of scrolls (see Fig. 2, a, d and Fig. 3, a-f).

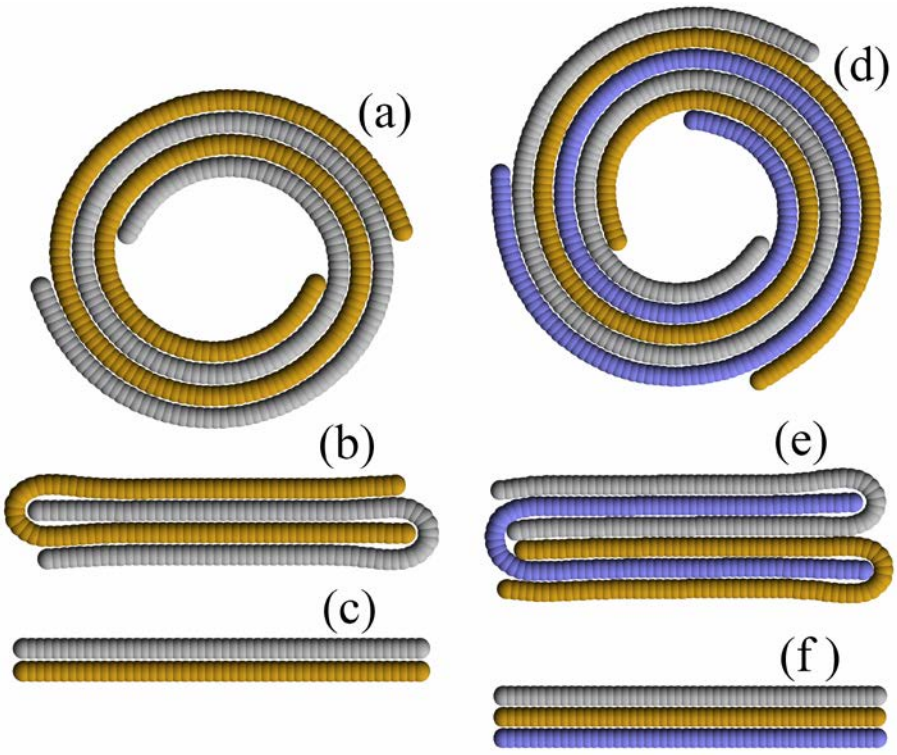

Fig. 2. (a) Symmetric scroll package of a double layered nanoribbon with length L=24.44 nm (number of nodes N=200). (b) Double fold of two nanoribbons with L=12.16 nm (N=100). (c) Flat double layered nanoribbon with length L=6.02 nm (N=50). (d) Symmetric scroll package of a three layered nanoribbon with length L=24.44 nm (N=200). (e) Double fold of three nanoribbons with L=12.28 nm (N=101). (f) Flat three layered nanoribbon with length L=6.02 nm (N=50).

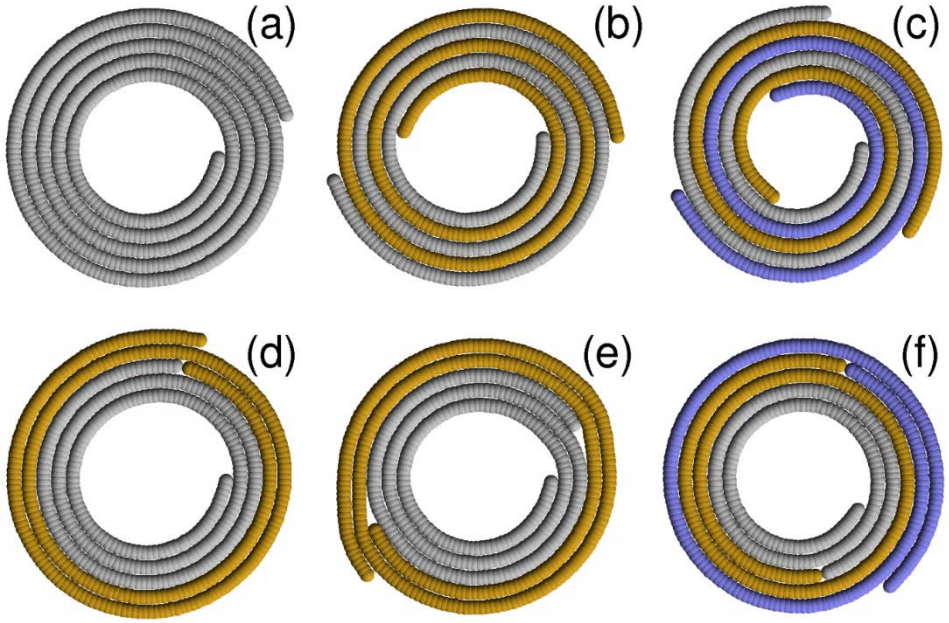

Fig. 3. (a) Scroll package of one nanoribbon with L=73.56 nm (number of nodes N=600). (b) Symmetric, (d) sequential and (e) opposite scroll package of two nanoribbons with length L=36.72 nm (N=300). (c) Symmetric and (f) sequential package of three nanoribbons with length L=24.44 nm (N=200).

4. Symmetric scrolls of several nanoribbons

The cross section of the symmetric scroll consisting of k nanoribbons has a shape of Archimedes spiral consisting of k equal chains (branches), see Fig. 2 a, d and Fig. 3 b, c. This structure is called symmetric because all nanoribbons are in equivalent configuration. There exist a number of possibilities of other scrolls, for example, combination of two spirals forming internal and external scrolls, namely, a system of embedded spirals (Fig. 3 d-f). The structure will be called sequential scroll package (Fig. 3 d, f) if all chains are twisted in one direction and opposite scroll (Fig. 3 e) in case of opposite twisting. The most convenient way to define the center of the spiral is considering its center of gravity:

$$u_0 = \frac{1}{Nk}\sum_{i=1}^{k}\sum_{n=1}^{N} u_{n,i}^0 ,$$

where $\left\{u_{n,i}^0\right\}_{n=1,i=1}^{N,k}$ is the solution of minimum problem (6) having a spiral shape and consisting of k chains (N is the number of nodes in each chain). In polar coordinate system one can define:

$u_{n,i,1}^0 = u_{0,1} + R_{n,i}\cos(\phi_{n,i})$, $u_{n,i,2}^0 = u_{0,2} + R_{n,i}\sin(\phi_{n,i})$,

where angle $\phi_{n,i}^0$ (phase of n-th node of i-th spiral) grows monotonously with increasing n. For a symmetric spiral consisting of k branches, one can find the radiuses $R_{n,1} = ... = R_{n,k}$ and the phases of neighbouring chain nodes $\left|\phi_{n,i+1} - \phi_{n,i}\right| = 2\pi / k$.

Symmetric k-chain spiral can be conveniently described by the number of coils of each chain:

$$N_c = \sum_{i=1}^{k}\left(\phi_{N,i} - \phi_{1,i}\right) / 2\pi k .$$

In case of big number of coils the spiral has a shape of a disc with internal void, see Fig. 3 (b) and (c). Border of the internal void is defined by chain nodes with numbers $n<n_1$, where n_1, – is the maximal node number n when $\phi_{n,i} - \phi_{1,i} < 2\pi / k$. Therefore, the radius of internal void can be written as:

$$R_1 = \frac{1}{kn_1}\sum_{i=1}^{k}\sum_{n=1}^{n_1} R_{n,i} \ .$$

External border of the spiral are set by the nodes numbered $N - n_2 < n \le N$, where n_2 – is the minimal value of node number n when $\phi_{N,i} - \phi_{n,i} > 2\pi / k$, so the external spiral radius is equal to

$$R_2 = \frac{1}{(N - n_2 + 1)k}\sum_{i=1}^{k}\sum_{n=N-n_2}^{N} R_{n,i} \ .$$

At first, let us consider a double layered nanoribbon, i.e. a system of two chains (k=2). The cross section of this configuration presents a symmetric double layered spiral (see Fig. 2 a). Dependence of normalized energy of the nanoribbon on its length L=(N-1)a for different configurations is shown in Fig. 4. A double fold of double layered nanoribbon is stable only in case of its length L>4.54 nm, its symmetric package can be realised only for nanoribbons with L>4.30 nm. Flat state of double layered nanoribbon is the most energetically favourable with length L<15.23 nm, while for larger length symmetric scroll configuration possesses the minimal energy. A folded state of double layered nanoribbon always has higher energy than that of the scroll package.

The rigidity of a double layer scroll is characterised by the lowest frequencies $\omega_1 < \omega_2 < \omega_3 < \omega_4$ of its natural vibrations. For a symmetric double chained spiral these vibrations correspond to periodical shifts of weakly deformed spiral branches relatively to each other. Dependence of coil number N_c, internal R_1 and external R_2 radii, four lowest natural vibration frequencies of a double layered nanoribbon scrolls on their length L are shown in Fig. 5. One can conclude that the coil number of double symmetric scroll grows proportionally to $L^{0.6}$, while the the internal and external radii obey the law $L^{0.23}$ and $L^{0.47}$, respectively, and frequencies decrease proportionally to L^{-1}.

Symmetric three layered nanoribbon in its cross section presents a symmetric three branch spiral, Fig. 2 d. The dependence of normalised energy E_0 for different stationary states of three layered nanoribbon on its length L=(N-1)a are shown in Fig. 6. Flat state of three layered nanoribbon is stable for all length values, double folded state can only exist with lengths L>4.79 nm, scrolled package can be realised with L>3.07 nm. In the case of L<16.30 nm, flat configuration is the most energetically preferable, while for longer structures the lowest energy has the scrolled structure. One should mention that a double fold of three layer nanoribbon always possesses higher energy in comparison to the scrolled state.

The rigidity of the three-chain spiral is characterized by the four lowest frequencies of its natural vibrations $\omega_1 < \omega_2 < \omega_3 < \omega_4$. The dependence of the number of coils, N_c, inner R_1 and outer R_2 radii, and the four lowest natural vibration frequencies of triple scroll on the nanoribbon length L are shown in Fig. 7. As it can be seen from the figure, number of coils in the scroll increases as the $L^{0.6}$, the internal and external radii grow as $L^{0.26}$ and $L^{0.48}$, and the lowest frequencies decrease as L^{-1}.

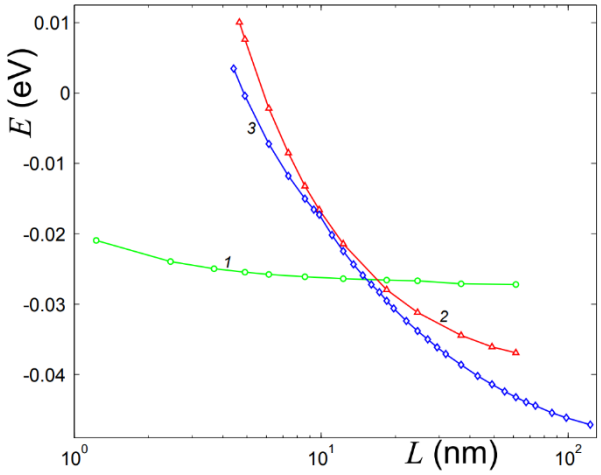

Fig. 4. Dependence of normalised energy on the length of the double layered nanoribbon for the case of flat configuration (curve 1), double fold (curve2) and symmetric scroll (curve 3).

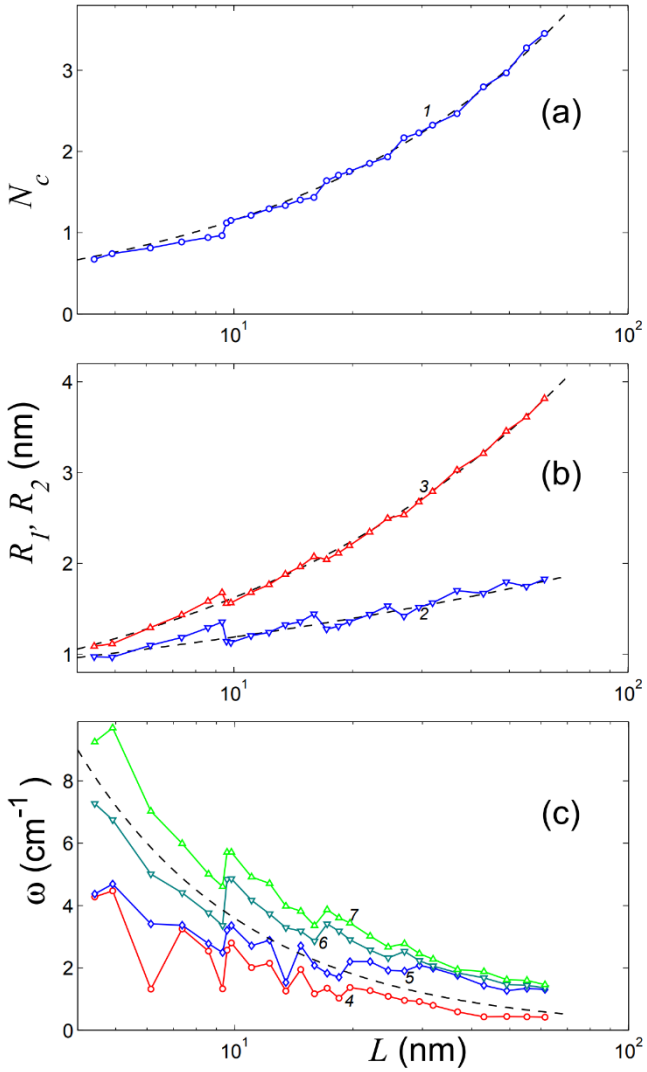

Fig. 5. Characteristics of stationary double-layered scroll as the functions of nanoribbon length L. (a) Number of coils N_c (curve 1), (b) internal R_1 and external R_2 scroll radii (curves 2 and 3), (c) four lowest natural vibration frequencies $\omega_1 < \omega_2 < \omega_3 < \omega_4$ (curves 4, 5, 6 and 7). Dashed lines show the following approximations: N_c=0.29$L^{0.6}$, R_1=0.7$L^{0.23}$, R_2=0.55$L^{0.47}$, ω=36/L.

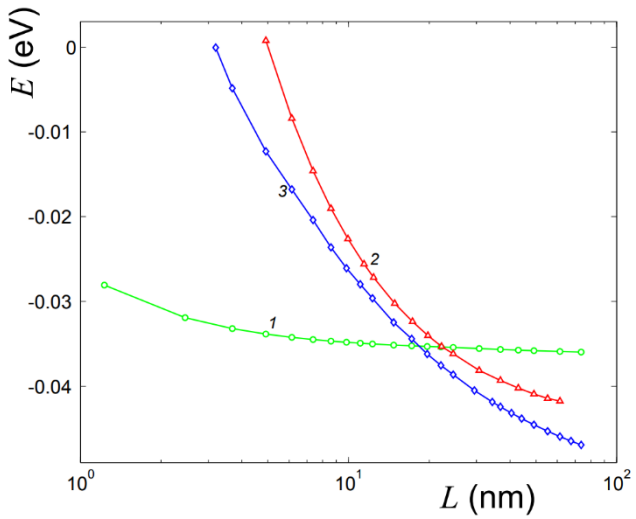

Fig. 6. Dependence of normalised energy of the three-layered nanoribbon E on its length L for the case of flat configuration (curve 1), double fold (curve 2), and symmetric scroll (curve 3).

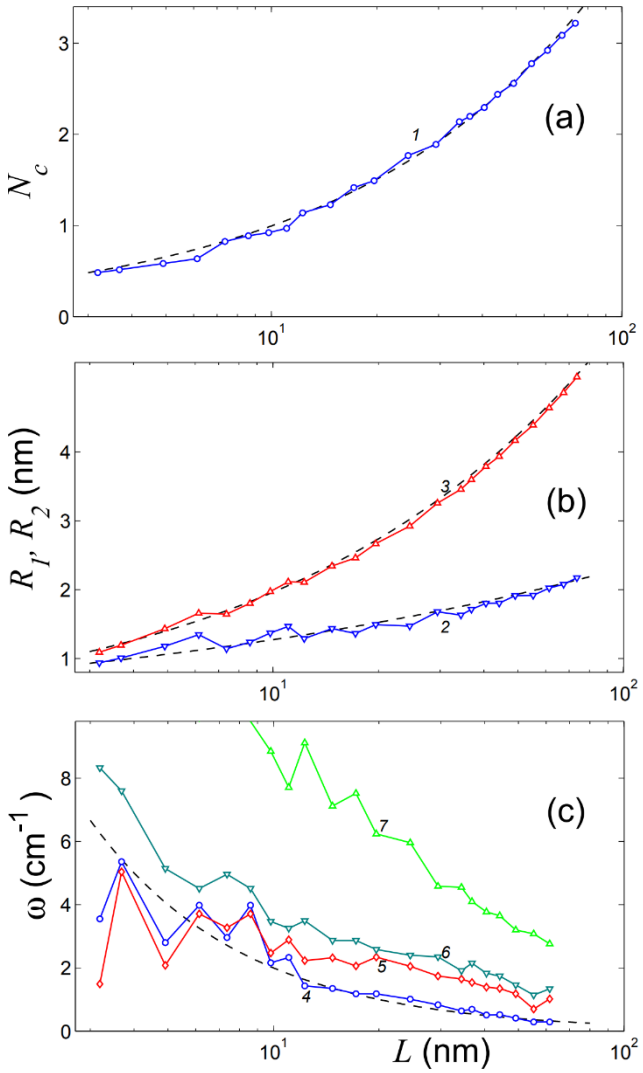

Fig. 7. Characteristics of equilibrium triple-layered scrolls on length L. (a) Coil number N_c (curve 1). (b) Internal R_1 and external R_2 scroll radii (curves 2 and 3). (c) Four lowest natural vibration frequencies $\omega_1 < \omega_2 < \omega_3 < \omega_4$ (curves 4, 5, 6 and 7). Dashed lines show the following approximations: $N_c=0.25L^{0.6}$, $R_1=0.7L^{0.26}$, $R_2=0.65L^{0.48}$, $\omega=20/L$.

5. Thermal expansion of multi-sheet scrolls

Let us use the Langevin system of equations for modelling of thermal vibrations of multi-layered scrolls,

$$M\ddot{u}_{n,j} = -\frac{\partial H}{\partial u_{n,j}} - \Gamma M\dot{u}_{n,j} + \Xi_{n,j} \qquad (7)$$

n=1,2,…,N, j=1,2,…,k,

where the vector $u_{n,j}=(x_{n,j}, y_{n,j})$ sets the coordinates of n-th particle of j-th chain H – is the Hamiltonian of the molecular system (5), k is the number of chains, N is the number of particles in each chain, the friciton coefficient $\Gamma=1/t_r$ (time of velocity relaxation t_r=5 ps), and $\Xi_{n,j}=(\xi_{n,j,1}, \xi_{n,j,2})$ is 2D vector of random forces with normal distribution, normalized by the following condition:

$$\left\langle \xi_{n,k,i}(t_1)\xi_{m,l,j}(t_2)\right\rangle = 2M\Gamma k_B T\delta_{nm}\delta_{kl}\delta(t_1-t_2),$$

where k_B is the Bolzman constant.

The system of equations of motion (7) was integrated numerically using the stationary state of the scrolls as the initial conditions. Stability of the scroll depends on the nanoribbon length, the longer are the nanoribbons, the more energy is gained by its coiling. Due to this fact, resistance of scrolls to thermal vibrations should increase with increasing nanoribbon length.

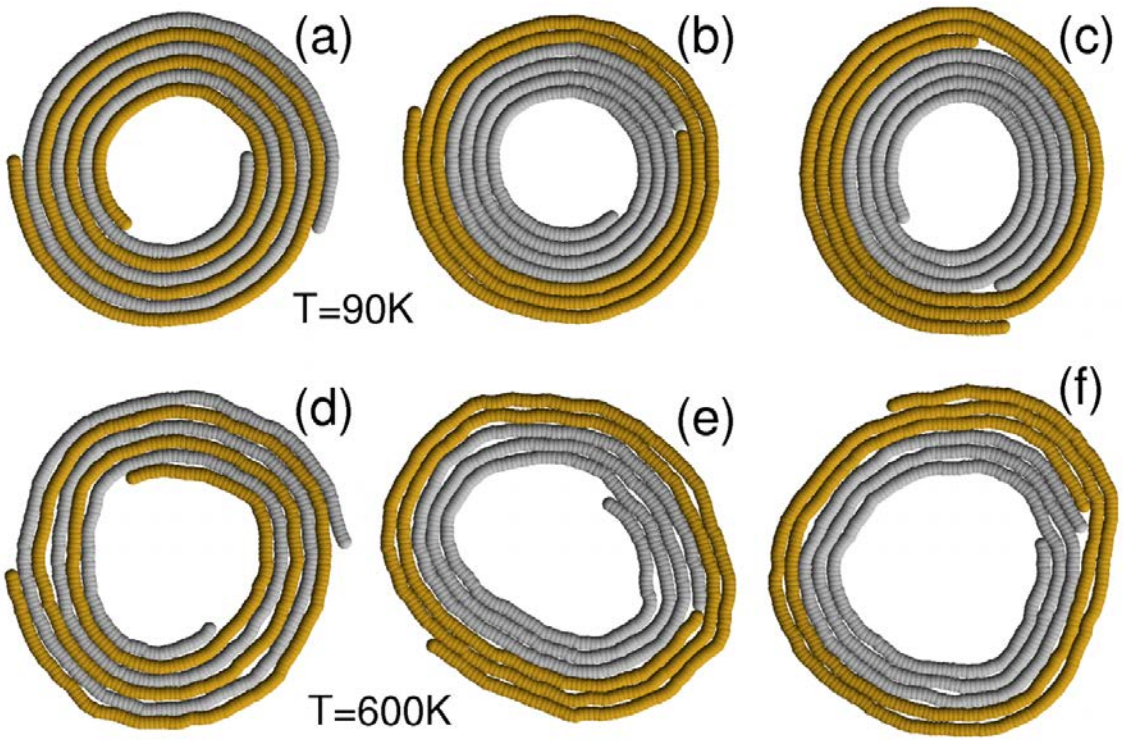

Fig. 8. Typical structure of two nanoribbon scrolls with length L=55.14 nm (number of chain nodes N=450) at the temperature T=90 K (top figures) and 600 K (bottom figures) for (a), (d) symmetric; (b), (e) sequential and (c), (f) opposite scrolls.

Let us consider dynamics of three possible configurations of two nanoribbon scrolls with N=450, k=2 and total number of particles $N\times k$ =900 with length $L=(N-1)a$=55.14 nm in the temperature interval 30<T<960 K. Numerical modelling of structure dynamics revealed that the configuration of the scroll remains stable in the mentioned temperature interval and they undergo thermal expansion. Typical shape of the scrolls are shown in Fig. 8 at T=90 K (top figures) and 600 K (bottom figures). As one can see from the fugure, topology of two-nanoribbon scrolls does not change with temperature, while geometrical parameters are

modified (decrease of coil number and growth of inner and outer radii with increasing temperature is observed).

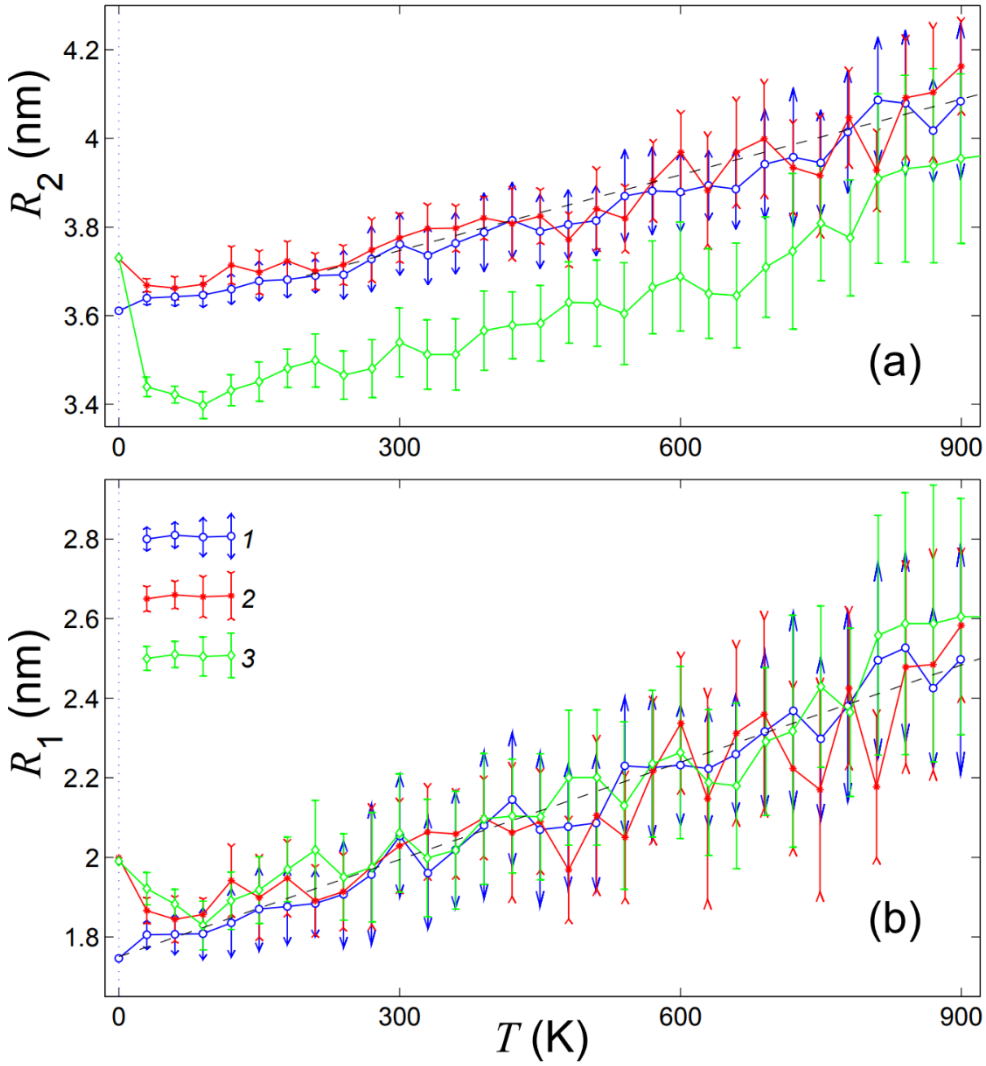

Fig. 9. Dependence of scroll characteristics on temperature T. (a) Average value of outer radius R_2 and (b) inner radius R_1 of two nanoribbon scrolls with L=55.14 nm (number of chain nodes N=450). Curve 1 presents the dependence for symmetric package, curve 2 is for sequential one, while curve 3 stands for opposite nanoribbon scroll. Dashed lines show the linear approximations of the numerical data.

Equilibrium between the thermostat and scroll structures is acheieved in time t=1 with steady scroll shape formation. By integration of equations of motion one can find averaged radii R_1, R_2 describing the scroll structure at given temperature. Their dependences on the temperature are shown in Fig. 9. The results reveal the monotonic growth of symmetric scroll radii with temperature. In low temperature range T<90 K thermal vibrations of sequential and opposite scrolls result in insignificant decrease of the radii. At higher temperatures the radii grow for all considered types of scrolls keeping the same thermal expansion coefficient, which can be astimated as $c_1 = d\langle R_1\rangle / dT = 0.0008$ nm/K for inner radius and $c_2 = d\langle R_2\rangle / dT = 0.0005$ nm/K for outer radius. Note that these values of linear thermal expansion coefficient are two or even three orders of magnitude higher than that of diamond.

An interesting aspect application of the chain model is taking into account the effect of the substrate. In our recent work this was done for the nanoscroll and it was revealed that

presence of the substrate shifts the spectrum of small amplitude phonon waves towards higher frequencies and stabilises the nanoscroll with respect to thermal fluctuations.

6. Conclusions

Chain model offered in [21] to describe secondary structures of graphene nanoribbons was extended here to describe static equilibrium structures as well as dynamics of multi-layered graphene nanoribbons. The model takes into account tensile and flexural rigidity of the nanoribbons together with the van der Waals interactions. It is shown that for sufficiently long nanoribbons, symmetric double- or triple-layered scrolls have lower energy as compared to flat configuration or to folded configuration.

Radial thermal expansion of the symmetric, sequential, and opposite double-scrolls was calculated and it was found that it is two or even three orders of magnitude larger than the linear thermal expansion coefficient of diamond. Such a large linear thermal expansion coefficient of nanoscrolls can be explained by considering the lowest frequency vibrational modes of scrolls. The mode with the lowest frequency is the twisting/untwisting mode [23], which is related to the change of the scroll diamiter. Since in thermal equilibrium all normal modes share equal energy which is proportional to squared amplitude times squared frequency, smallness of frequency means large vibration amplitude. Thus, the low frequency twisting/untwisting mode has a very large amplitude, explaining the anomaloysly large coeffisint of radial thermal expansion of the graphene nanoribbon scrolls.

Very high radial koefficient of thermal expansion makes carbon nanoscrolls very promising for making sencitive thermal sensors.

Our results demonstrate the efficiency of the chain model in atomistic simulations of secondary structures of graphene nanoribbons.

Acknowledgements. *A.V. Savin thanks financial support provided by the Russian Science Foundation, grant No. 14-13-00982, and the Joint Supercomputer Center of the Russian Academy of Sciences for the use of computer facilities. E.A. Korznikova is grateful for the financial support from the Russian Foundation for Basic Research (grant No. 17-02-00984). S.V. Dmitriev acknowledges financial support provided by Russian Science Foundation, grant No. 16-12-10175.*

References

[1] A.K. Geim, K.S. Novoselov // *Nat. Mater.* **6** (2007) 183.
[2] Y.K. Kim, K.S. Kim // *Nat. Nanotechnol.* **3** (2008) 408.
[3] Y. Gao, W. Yang, B. Xu // *Carbon* **96** (2016) 513.
[4] Y. Doi, A. Nakatani // *Journal of Solid Mechanics and Materials Engineering* **6** (2012) 71.
[5] J.A. Baimova, S.V. Dmitriev, K. Zhou // *Europhys. Lett.* **100** (2012) 36005.
[6] E.A. Korznikova, A.V. Savin, J.A. Baimova, S.V. Dmitriev, R.R. Mulyukov // *JETP Lett.* **96** (2012) 222.
[7] E.A. Korznikova, J.A. Baimova, S.V. Dmitriev // *Europhys. Lett.* **102** (2013) 60004.
[8] A. Shahabi, H. Wang, M. Upmanyu // *Sci. Rep.* **4** (2014) 7004.
[9] L. Yang, P. Cheol-Hwan, Y-W. Son, M.L. Cohen, S.G. Louie // *Phys. Rev. Lett.* **99** (2007) 186801.
[10] W. Bollmann, J. Spreadborough // *Nature (London)* **186** (1960) 29.
[11] J. Spreadborough // *Wear* **5** (1962) 18.
[12] M.V. Savoskin, V.N. Mochalin, A.P. Yaroshenko et al. // *Carbon* **45** (2007) 2797.
[13] X. Xie, L. Ju, X. Feng // *Nano Lett.* **9** (2009) 2565.
[14] D. Roy, E. Angeles-Tactay, R.J.C. Brown // *Chem. Phys. Lett.* **465** (2008) 254.
[15] S.S. Datta, D.R. Strachan, S.M. Khamis, A.T. Jonson // *Nano Lett.* **8** (2008) 1912.

[16] R. Rurali, V.R. Coluci, D.S. Galvao // *Phys. Rev. B.* **74** (2006) 085414.
[17] V. Barone, O. Hod, G.E. Scuseria // *Nano Letters* **6** (2006) 2748.
[18] E.L. Aero // *Advances in Mechanics* **1** (2002) 131.
[19] E.L. Aero // *Journal of Engineering Mathematics* **55** (2006) 1.
[20] A.V. Porubov, E.L. Aero, G.A. Maugin // *Phys. Rev. E* **79** (2009) 046608.
[21] A.V. Savin, E.A. Korznikova, S.V. Dmitriev // *Phys. Rev. B* **92** (2015) 035412.
[22] A.V. Savin, E.A. Korznikova, S.V. Dmitriev // *Phys. Solid State* **57** (2015) 2348.
[23] A.V. Savin, E.A. Korznikova, S.V. Dmitriev // *Letters on Materials* **6** (2016) 77.
[24] A.V. Savin, E.A. Korznikova, I.P. Lobzenko, Y.A. Baimova, S.V. Dmitriev // *Phys. Solid State* **58** (2016) 1278.
[25] A.V. Savin, E.A. Korznikova, S.V. Dmitriev, E.G. Soboleva // *Comp. Mater. Sci.* **135** (2017) 99.
[26] A.V. Savin, Yu.S. Kivshar, B. Hu // *Phys. Rev. B* **82** (2010) 195422.
[27] A.V. Savin, Yu.S. Kivshar // *Phys. Rev. B* **81** (2010) 165418.
[28] S.V. Dmitriev, E.A. Korznikova, J.A. Baimova, M.G. Velarde // *Phys. Usp.* **59** (2016) 446.
[29] I. Evazzade, I.P. Lobzenko, E.A. Korznikova, I.A. Ovid'ko, M.R. Roknabadi, S.V. Dmitriev // *Phys. Rev. B* **95** (2017) 035423.